Hearing Research 426 (2022) 108626

Contents lists available at ScienceDirect

Hearing Research

journal homepage: www.elsevier.com/locate/heares

Research Paper

Structural changes in the human stria vascularis induced by aminoglycosides and loop diuretics

Anthony Wright*, Andrew Forge, Daniel J. Jagger

UCL Ear Institute, University College London, 332 Gray's Inn Road, London, WC1X 8EE, United Kingdom

ARTICLE INFO

Article history:
Received 28 April 2022
Revised 5 September 2022
Accepted 30 September 2022
Available online 2 October 2022

Keywords:
Stria vascularis
Human
Ototoxicity
Aminoglycosides
Loop diuretics
Hearing loss
Deafness

ABSTRACT

The human stria vascularis has been examined both by scanning and transmission electron microscopy in normal controls and from individuals who had received loop diuretics, aminoglycoside antibiotics or some combination of the two prior to their deaths. The tissues were preserved by perilymphatic perfusion of fixative within an hour of death and preservation was adequate. The normal ultrastructure is described and does not differ significantly from that found in experimental animals. The loop diuretics are associated with structural changes that cannot be distinguished from those found in animals treated with large doses of the same drugs. The aminoglycosides caused some changes, but the patients had been in renal failure and this probably contributed to the structural alterations. The combination of a loop diuretic and aminoglycoside was associated with a range of alterations from mild to severe. Overall, the three treatment groups had a series of ultrastructural changes resembling those found in animal models thereby justifying the use of experimental animals to predict human ototoxicity.

1. Introduction

Experimental animals are used in ototoxicity research for two major purposes. First, to allow the exploration of the mechanism of action of the ototoxic effect and second to act as model systems to anticipate a damaging effect in humans. For this second purpose, healthy animals are usually given large doses of a drug, often over a short period of time, and if structural or physiological changes are subsequently detected in the cochlea, then it is usually assumed that similar changes are likely to occur in humans. There are several problems with making such assumptions as different species handle, or are affected by, the same drug in a variety of ways. Some of these species differences have been clearly shown during the early work with dihydrostreptomycin and its action on the organ of Corti. The drug is profoundly toxic to humans (Shambaugh et al., 1959), causes severe damage to the Patas monkey cochlea at low dose levels (Hawkins et al., 1977), and slight damage to the cat at huge doses (Hawkins and Lurie, 1953; McGee, 1961) yet does not seem to affect the guinea pig at all (Hawkins, 1976). Thus lack of an effect in one species does not confer safety in another, although when damage does occur in the experimental animal great care should be exercised when the drug is used in humans.

Two major classes of drugs with ototoxic side effects are available to the medical profession. Cochleotoxic aminoglycoside antibiotics cause more damage to the organ of Corti with some changes in the stria vascularis (SV) (Forge and Schacht, 2000), whilst loop diuretics predominantly affect the SV with no or minimal changes in the organ of Corti (Ding et al., 2016). For animal models to be reliable and useful predictors of human ototoxicity then at some time changes should have been seen in the human cochlea that resemble those found in experimental animals. Unfortunately, there are few if any ultrastructural studies of the effects of the aminoglycosides on the human cochlea, although there are many that have used light microscopy to view sections or surface preparations.

There are few temporal bone reports of patients who had received loop diuretics prior to their deaths (Matz et al., 1969; Meriwether et al., 1971; Matz, 1976). The only ultrastructural survey of the human cochlea in a well-documented case of hearing loss secondary to large doses of furosemide (also known as frusemide) and ethacrynic acid was described by Arnold and colleagues (Arnold et al., 1981). The patient, a 57 year old anuric man, developed a 80-90 dB sensorineural hearing loss across all frequencies examined 5 days after the administration of 5000 mg of frusemide and 200 mg of ethacrynic acid for profound renal failure. Some six years earlier he had received both streptomycin

* Corresponding author.
E-mail address: Anthony.Wright@ucl.ac.uk (A. Wright).

https://doi.org/10.1016/j.heares.2022.108626

(30g) and capreomycin (27g). The cochlea was preserved by perfusion 30 minutes after death. The ultrastructural findings in this single case were like those found in animals receiving loop diuretics. In the SV the major features were enlargement of the intercellular spaces and an apparent shrinkage of the marginal and intermediate cells. However, Merck and colleagues showed that experimental renal failure induced by sub-total nephrectomy also causes ultrastructural changes in the SV similar to those seen with the loop diuretics (Merck et al., 1976). Thus Arnold's work, whilst an extremely valuable addition to the literature and the first report of ultrastructural changes in the human, must be interpreted as showing the effects of the administration of loop diuretics in the presence of severe renal failure and not of the loop diuretics alone.

The major reason for a lack of human material suitable for electron microscopy is the difficulty in obtaining adequate fixation of fine structures before post-mortem autolysis causes alterations that often cannot be distinguished from pathological change (Wright, 1980a). The purpose of the work described in this paper was to evaluate the ultrastructural changes, if any, that arose in the SV of well-preserved temporal bones from patients who had received aminoglycosides, loop diuretics or some combination of the two, prior to their deaths and to compare them with controls who had not received these drugs.

2. Material and methods

2.1. Human cochlear tissue preparation and electron microscopy

Procedures were performed in accordance with the UK legislation in force at the time; in the UK in the 1980s, the standard hospital postmortem form allowed for removal of tissues other than for the purposes of transplantation provided the relatives' consent had been obtained. Appropriate consent was obtained for all samples used in this study.

The striae from 21 patients were examined. Table 1 describes the patients and their medical information (including drugs given, blood analysis and renal status). Eight were controls and did not receive any ototoxic drugs. The other 13 received either an aminoglycoside (2 patients), a loop diuretic (6), or some combination of the two (5). Some of the patients were in renal failure and some had audiograms prior to their death. In the treatment group two patients had audiograms (Table 2) and these were prior to treatment. All the audiograms were better than the 75th percentile of Robinson and Sutton's data for age and sex matched normal individuals (Robinson and Sutton, 1979). Those without audiograms had no history of hearing difficulties nor any history of hearing loss. All had normal tympanic membranes and middle ears. As the patients were in hospital their haematological status was maintained as close to normal as possible although in subjects 10, 14, 20 and 21 the haemoglobin did drop to below 10 g/dl. Apart from those in renal failure, blood urea and electrolytes were also within the normal range (Table 1).

Cochlear fine structure was preserved within 1 hour of death. The fixative was 2.5% glutaraldehyde and 2% formaldehyde in 0.15 M sodium cacodylate buffer with 3mM calcium chloride at pH 7.25. The osmolarity of the buffer was 289 mOsm/l and of the completed fixative was 1205 mOsm/l as measured by freezing point depression. A tympano-meatal flap was raised, the stapes displaced and the fixative perfused through the round window. Both windows were sealed and at post mortem a block of temporal bone containing the labyrinth was removed and stored in fixative. The membranous labyrinth was post fixed and stained for 1h with 1%

Table 1
Patient clinical data.

Patient	Age	Sex	AG (mg)	Peak µg/ml	LD IV (mg)	Urea mmol/li	Creat. µmol/li	Hb (g/dl)	Clinical
1	69	F	-		-	2.9	63	13.1	Transglottic Ca. VCR, MT, Bl, 5FU
2	59	F	-		-	4.5	75	12.7	Transglottic Ca. RT
3	62	M				3.4	84	13.5	Laryngeal Ca. Laryngectomy. Bilateral Neck Dissection
4	63	M				10.1	199	13.6	Laryngeal Ca. Rt. Laryngectomy, Thyroidectomy. Pre terminal Renal failure
5	62	M	-		-	4.6	77	12.8	Tonsillar Ca. Lung 2°. RT. Neck Dissection. MI
6	53	M				NA	NA	NA	Duodenal bleed, Hypothermia, MI
7	71	M	-		-	8.8	98	14.4	Buccal Ca. RT, Neck Dissection
8	46	M	-		-	48.4		13.1	Tonsillar Ca. Lung 2°. VCR, MT, Bl, 5FU, Cyc. Rifa. Isona
9	63	M	G 540	16.3		45.0 max		c10	Leaking aortic aneurysm, anuria, Peritonitis, Dialysis
10	50	M	G 1520	15.7		58.0 max	905 max	c10	Pneumonia, Hyponatraemia, Renal and Hepatic failure
11	52	M	-		B 34			12.4	Skull base lesion. RT. SVT
12	59	M	-		F 80	8.4		14.7	Respiratory Failure. Cor Pulmonale. Death in 4h
13	39	M	-		F 140	4.8	142	16.6	Sub arachnoid Hh. 100mg Frusemide 10min prior to death
14	77	M			F 160 B 4	NA	NA	8.4	Acute LVF. No History heart disease. IV Loops within 4h of death
15	64	F	-		F 1100	6.4	NA		MI. Iv Frusemide over 12h prior to death
16	73	M	-		F 235	11.6 max	NA		Post Cricoid Ca. 120 mg Frusemide 4h pre death
17	25	F	G 1160		F 600	12.8		12.1	Ruptured Ectopic. Pulmonary oedema
18	71	M	G 1960		F 350 B 2	32.0 max		10.6	Pneumococcal Pneumonia, DIC, Dialysis
19	68	F	T 1200 G 4080	 6.75	B 22	19.9 max	175 max	11.8	Post Cricoid Ca. Stomach pull up. Septicaemia
20	20	F	T 560		F 60 B 6.5	3.2	61	11.8	Takayashu's ds. Arterial bypass surgery. Pneumonia
21	58	F	T 980	11.4	F 40 B 8	17.3 max	270 max	12.1	Pneumonia. Tension Pneumothoraces.

Abbreviations: AG, Aminoglycoside; LD, Loop diuretic; F, Frusemide; B, Bumetanide; G, Gentamicin; T, Tobramycin; Ca., Carcinoma; VCR, Vincristine; MT, Methotrexate; Bl, Bleomycin; 5FU, 5 Fluorouracil; RT, Radiotherapy; MI, Myocardial infarct; Rifa, Rifampicin; Isona, Isoniazid; SVT, Supra Ventricular Tachycardia; Hh, Haemorrhage; LVF, Left Ventricular Failure; DIC, Disseminated Intravascular Coagulopathy.

Table 2
Patient audiometric data.

Pure Tone, Masked Bone Conduction Thresholds (dB SPL)								
Patient	Right ear				Left ear			
	0.5 kHz	1 kHz	2 kHz	4 kHz	0.5 kHz	1 kHz	2 kHz	4 kHz
2	35	45	40	50	30	35	35	35
3	15	20	45	60	15	15	40	60
4	15	0	15	50	15	0	15	40
5	10	5	10	40	15	5	5	35
7	0	5	20	30	0	10	45	50
8	5	0	0	15	5	5	10	25
19	10	5	20	35	0	0	20	35

osmium tetroxide in buffer after a buffer wash, both solutions being perfused through the round window. The osmium was washed out with buffer and 50% then 70% ethanol was perfused through the cochlea. The block of bone was stored in 70% ethanol until dissection.

The bony labyrinthine capsule was drilled away until only a thin shell remained over the membranous labyrinth. Starting at the apex, this bone was removed to expose the scala media. Reissner's membrane was removed and the SV dissected out in short strips starting at the apex. Each strip was divided into two portions which were subsequently processed for either transmission or scanning electron microscopy.

For scanning electron microscopy (SEM) the specimens were dehydrated through ethanol in steps of 80%, 95%, 100% and a repeat of the 100%, each step taking 10 min. A Polaron E-3000 critical point drier was used to dry the specimens from liquid CO_2. The specimens were subsequently mounted on specimen stubs and coated with gold and palladium in an Edwards 360 vacuum coating unit with a rotary stage. A Jeol 35c scanning electron microscope was used to view the specimens.

For transmission electron microscopy (TEM) each portion was block stained with uranyl acetate in 70% ethanol for 30 min. The specimens were dehydrated through an ethanol series (95%, 100%, 100% ethanol stored over anhydrous copper sulphate) and passed through two 15 min. changes of propylene oxide before embedding in TAAB resin. Semi thin sections were stained with toluidine blue and ultrathin sections with uranyl acetate and lead citrate. An A.E.I. 802 or Jeol 100S transmission electron microscope was used to examine the specimens.

3. Results

To provide a context for the results from the human SV, a diagram depicting its structure as derived from observations of animals is presented in Fig. 1A, and an image of the SV of the normal mouse in Fig. 1B. The SV in animals is formed of three closely apposed cell types and enclosing a capillary network. Marginal cells (MC) line the endolymphatic space. Extensive infoldings of the basal aspect of the cell project through the body of the tissue. These infoldings enclose large mitochondria. Marginal cells are active ion transporter cells, pumping potassium into endolymph. Intermediate cells (IC) are entirely enclosed within the body of the SV and interdigitate with marginal cell infoldings. Intermediate cells play a crucial role in the generation of endocochlear potential (EP) (Steel and Barkway, 1989). Basal cells (BC) separate SV from the underlying spiral ligament (Souter and Forge, 1998). Tight junctions between basal cells provide a permeability barrier from the intercellular spaces of the spiral ligament, ensuring electrochemical isolation of the intercellular spaces of SV from the underlying tissues. The capillary lumen is surrounded by endothelial cells (end), the intercellular spaces of which are sealed by tight junctions. Pericytes (pc), which are contractile, appose the outer surface of the endothelial cells. Endothelial cells and pericytes are enclosed within the capillary basement membrane. Processes of marginal cells and intermediate cells contact the outer surface of the capillary basement membrane. An additional cell type that also contacts the capillaries, the perivascular macrophage (not shown in these images), has also been described (Zhang et al., 2012).

3.1. The normal controls

The appearance of the SV in toluidine-blue stained sections the SV of patients who had received neither of the drugs under test and had normal audiograms for their age ("normal"; Fig. 2A, B), were similar. The endolymphatic surface of the SV was generally smooth and without any irregularity of the limiting membrane except for small blisters apparent in many of the sections (arrows and inset in Fig. 2A). The nuclei of the marginal cells were close to the endolymphatic pole of the cell and the strial capillaries tended to be filled with erythrocytes. In many sections, especially those taken from the apical portions of the cochlea, the stria was atrophic being replaced by a thin sheet of cells (Fig. 2C).

The surface features of the human SV as observed by scanning electron microscopy (SEM) have been previously described (Wright, 1980b), but in essence the surface of the stria was flat without any gross irregularity (Fig. 3A). The endolymphatic surface of marginal cells usually have a hexagonal outline which is often irregular and there is a wide variation in the free surface area.

Each marginal cell had microvilli on its surface and there was great intercellular variation in the density and size of these microvilli. Between the SV and the spiral prominence (Fig. 3B) was the transitional zone where the hexagonal cell outline of the marginal cells was replaced by an elongated diamond shape with the long axis running parallel to the long axis of the cochlear duct (Fig. 3B,C). The transitional cells had only scanty, short microvilli on their endolymphatic surface (Fig. 3C). Some specimens had blisters arising from the marginal cell surface usually close to the intercellular junction (Fig. 3A). This finding was sporadic in the control group occurring in different portions of the same specimen and being scattered throughout the length of the cochlea.

3.1.1. The marginal cells

Great variability was present amongst the marginal cells even in these normally hearing ears (Fig. 4A,B). The classic, darkly staining cell, as described in animal studies, is present in the human stria and corresponds to those areas of non-atrophied SV seen in the semi-thin sections. These normal marginal cells, which had a similar morphology throughout the SV, had a luminal surface and made contact with both the intermediate and basal cells as well as with the basement membrane of the capillaries.

The surface of many, but not all, of the typical marginal cells contained pinocytic invaginations, often in close proximity to small coated vesicles in the submarginal cytoplasm (Fig. 4A inset). At the tight junction between adjacent marginal cells at the endolym-

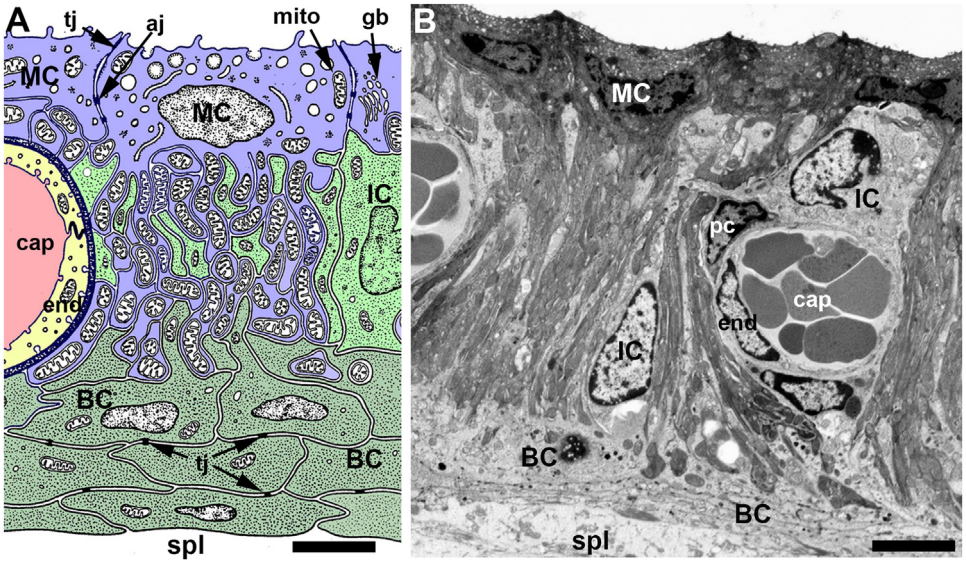

Fig. 1. Organisation of the mammalian stria vascularis. (A) Diagram of a cross-section of the SV of an animal to show the different cell types and their organisation. (B) Section of mouse SV imaged by transmission electron microscopy. Abbreviations: MC = marginal cells; IC = intermediate cell; BC = basal cell; cap = intraepithelial capillary; end = capillary endothelial cell; pc (in B) = pericyte, apposed to capillary endothelial cell; sp lig = spiral ligament that underlies the SV; tj = tight junction; aj = adherens junction; mito = mitochondrion; gb = golgi body. Scale bars: 5 µm.

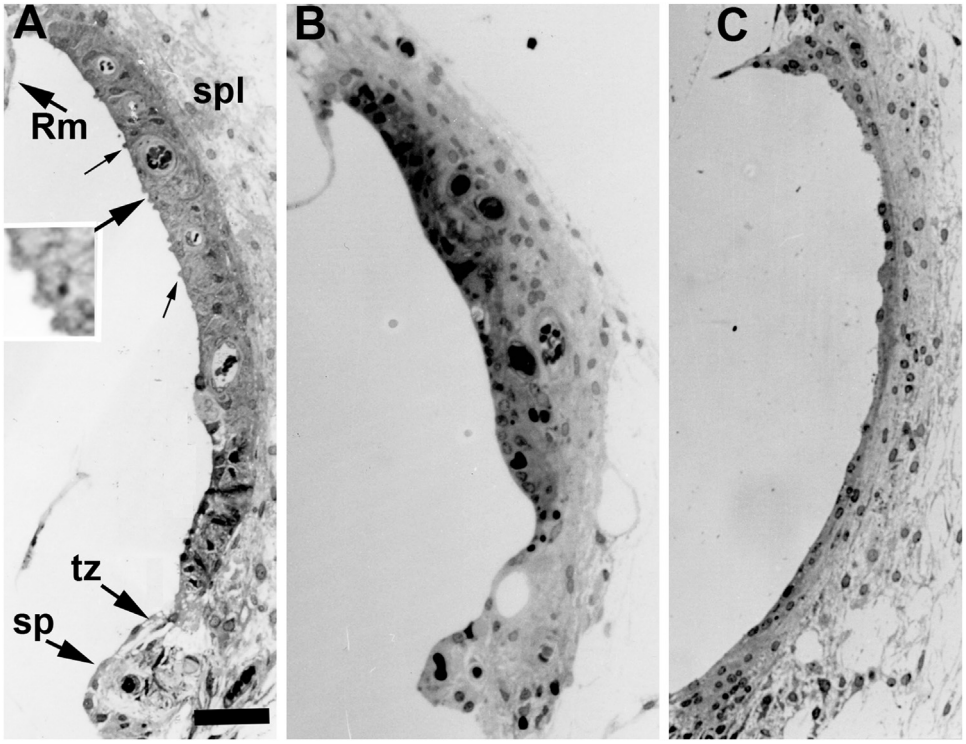

Fig. 2. Representative toluidine-blue stained sections of the stria vascularis. In each the remnant of Reissner's membrane is at the top of each micrograph (Rm in panel A). (A) Patient 3 (normal); mid-basal turn. Small arrows indicate blisters at the endolymphatic surface of marginal cells. Inset shows higher power view of blistering at the site in marginal cell surface indicated by the larger arrow. Abbreviations: tz = transitional zone; sp = spiral prominence. Scale bar: 50 µm, applies to all panels. (B) Patient 4 (normal); lower middle turn. (C) Patient 3 (normal) apical turn.

phatic surface (labelled tj in Fig. 4A,B), the membranes of adjacent cells were closely apposed and parallel; electron densities associated with the tight junction region were preserved, as were the cytoskeletal elements associated either side of the adherens junction in the apposed cells (Fig. 5A). The cytoplasm of the marginal cell comprised a darkly stained matrix packed with organelles. The mitochondria were large and numerous especially within the basal projections. They were compact with no swelling, the outer membrane regular in outline with no disruption or distortions, and the cristae formed by the inner membrane regularly arranged (Fig. 5B). Well-developed Golgi apparatus was often seen and was usually in the apical region of the cell (Fig. 4B). They showed typical asymmetric layering of lamellae that increased in thickness in one direction towards released vesicles on one side (Fig. 5C). Osmiophilic inclusions and granules with the morphological features of lipofuschin were found in some marginal cells (Fig. 4C), but were un-

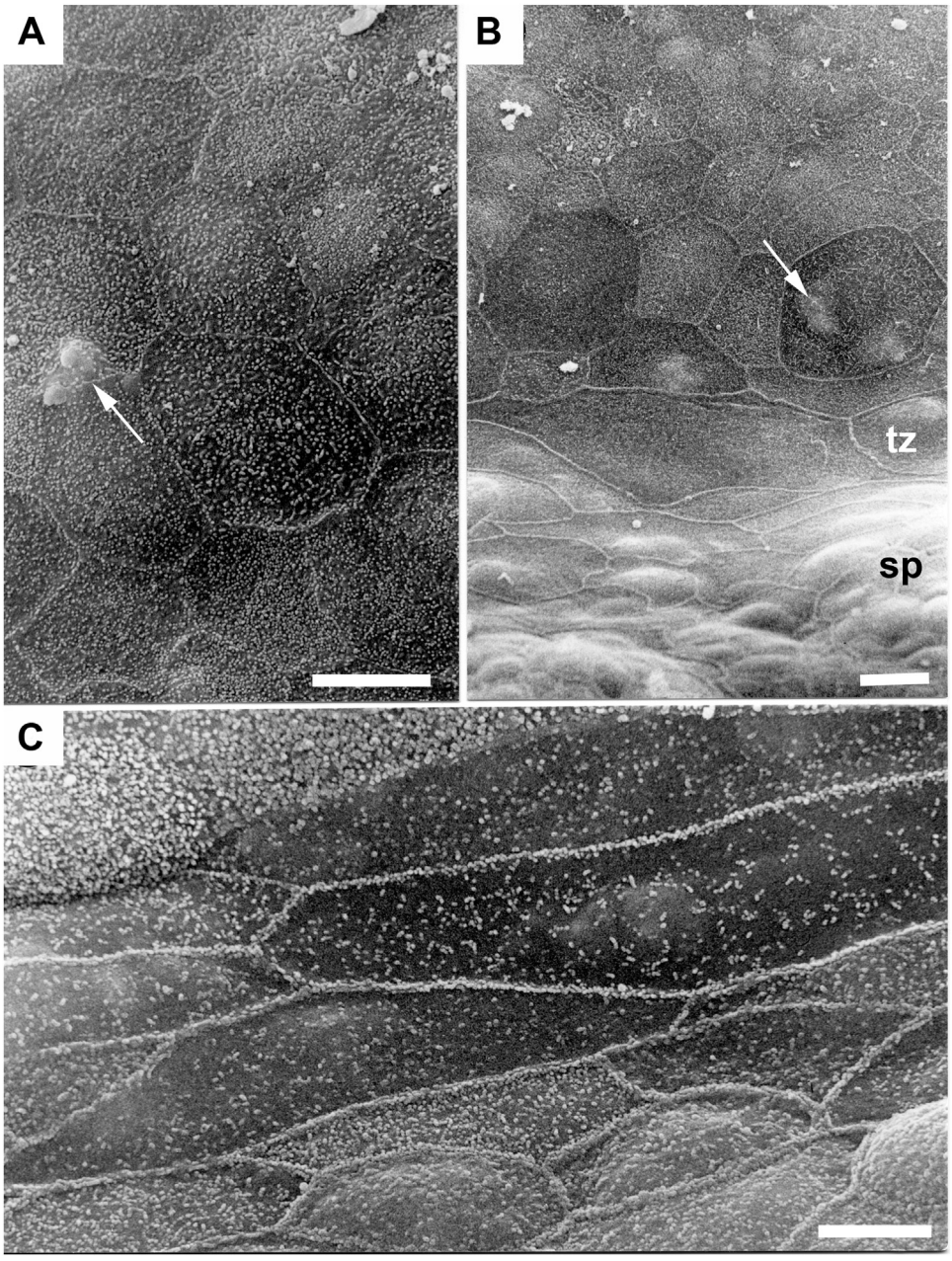

Fig. 3. Surface features of normal human stria vascularis visualised by scanning electron microscopy. (A) Patient 3; basal turn. The irregular hexagonal outlines of the endolymphatic surfaces of the marginal cells are clearly seen along with a profusion of microvilli. Arrow indicates blisters arising from the endolymphatic surface of a marginal cell. Scale bar: 5 μm. (B) Patient 3; middle turn. Junction of the SV with the spiral prominence (sp). Arrow indicates blister at apical surface of a marginal cell. The elongated cells of the transitional zone (tz) between the two levels are seen. Scale bar 10 μm. (C) Patient 2; apical turn. The elongated cells of the transitional zone with their scanty covering of microvilli are easily discernible from the smaller more compact cells of the spiral prominence. Scale bar: 5μm.

common. The marginal cell nucleus was multi-lobulated but was otherwise unremarkable.

The border with neighbouring marginal cells was well defined in the apical regions, but closer to the basal part of the cell that becomes highly convoluted and difficult to follow as a close relationship is established between adjoining marginal, intermediate and basal cells. It was difficult to determine how far a marginal cell extended in a basal direction, but projections appeared to reach the capillaries, where a basement membrane intervened (Fig. 4A), and with the basal cells (Fig. 4D).

3.1.2. The intermediate cells

The intermediate cells were fewer in number than the marginal cells and had a less densely stained cytoplasm (Fig. 4B, D). Mitochondria were fewer and smaller than those of marginal cells. Occasionally areas within the intermediate cells were found to be packed with rough endoplasmic reticulum and layers or whorls of smooth endoplasmic reticulum. The cell borders were highly convoluted, and like the marginal cell the extent of an individual intermediate cell was often difficult to assess. However, they could be traced to the capillaries (Fig. 4A) and their processes interdigitated not only with those of other intermediate cells but also with those of marginal and basal cells (Fig. 4D). Again, lipofuschin-like granules were sometimes present in intermediate cells (Fig. 4C).

3.1.3. The basal cells

The basal cells were flattened, long cells lying on the fibrocytes and fibrous bundles of the spiral ligament (Fig. 4D). Near to

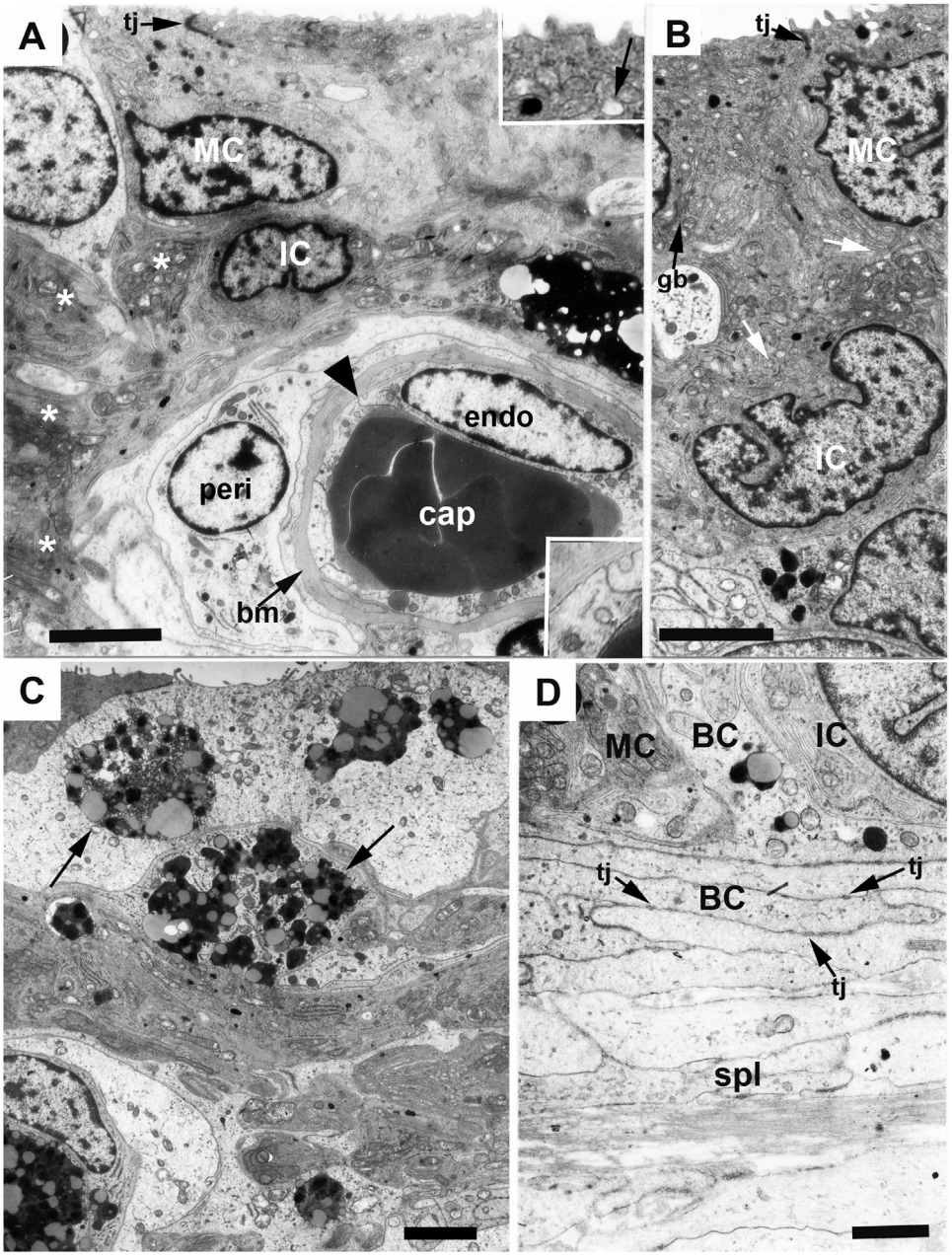

Fig. 4. Sections of stria visualised by transmission electron microscopy. In all the micrographs the endolymphatic surface is uppermost. (A) Patient 3 (normal); basal turn. Abbreviations: MC = marginal cell lining the endolymphatic space with complex basal infoldings (asterisks); IC = intermediate cell; cap-capillary lumen filled with red blood cells; endo = capillary endothelial cell; peri=capillary pericyte; bm = thick basement membrane surrounding capillary; tj = tight junction between adjacent marginal cells. Scale bar: 10μm. Inset at top shows apical pinocytotic vesicle opening to endolymphatic space and vesicle in apical cytoplasm of the marginal cell (arrow). Inset at bottom shows detail of endothelial cell at the large arrowhead in main figure, revealing a pinocytotic vesicle opening to the strial side of the capillary, and a coated vesicle close to the luminal side of the cell, with an intact tight junction between adjacent endothelial cells. (B) Patient 3 (normal); basal turn Marginal and Intermediate cells (MC, IC) with complex interfolding of the cell processes indicated by arrows. Scale bar: 10 μm. (C) Patient 6 (normal); basal turn. Electron dense, lipofuschin-like bodies are present in marginal cell (arrows). Scale bar: 2 μm. (D) Patient 4 (renal failure, RF); lower middle turn. Basal cells (BC), in two to three layers, have elongated cell bodies and those in the layer facing the rest of the stria have projections into the body of stria that contact intermediate cells (IC) and the extensively infolded basal projections of marginal cells (MC). There are tight junction-like punctate electron densities at points of close apposition between the adjacent basal cells (tj). On their basal aspect, the basal cells are apposed to the fibrocytes of the spiral ligament (spl). Scale bar: 5 μm.

the other strial cells, contact between neighbouring basal cells was tight with a barely discernible intercellular space and numerous punctate condensation at the cell membrane suggestive of tight junctions. These basal cells occasionally contained large granules with osmiophilic inclusions and lipoid bodies intermixed (Fig. 4D). Otherwise, the cytoplasm was usually pale-staining due to a relative paucity of organelles. Cell processes did extend up from the basal cells into the marginal and intermediate cell layer (Fig. 4D), but did not appear to be at all extensive. Towards the spiral ligament, the distinction between the fibrocytes of this region and the basal cells was often difficult. The fibrocytes became separated by wide intercellular spaces containing large amounts of fibrillar material in a loose matrix, although cohesion between cells of the spiral ligament was maintained. Small, puncta-like direct contacts between adjacent fibrocytes may have been gap junction plaques shown to be numerous between spiral ligament fibrocytes in animals (Jagger and Forge, 2015).

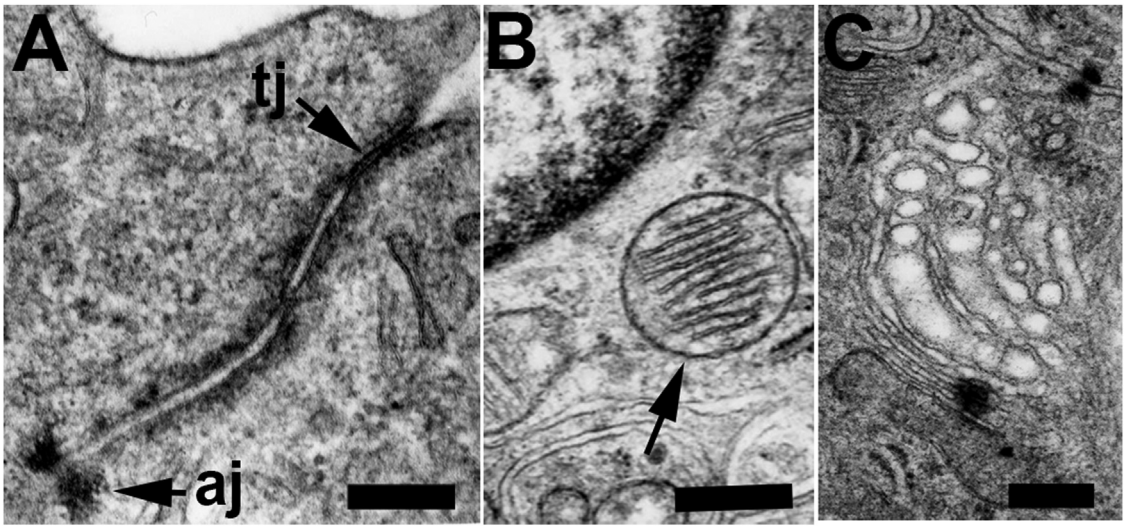

Fig. 5. Representative high resolution TEM images of subcellular structures in normal human stria vascularis. (A) Intercellular junction at the luminal surface between adjacent marginal cells. The plasma membranes of the adjacent cells are closely apposed, and parallel with a uniform intercellular spacing. Characteristic electron densities in each cell at site of the tight junction permeability barrier (tj), and cytoskeletal elements associated with the adherens junction (aj) clearly resolved. Scale bar: 0.1 μm. (B) Mitochondrion, arrowed, is compact with a regular, smooth outer membrane and the cristae formed by inner membrane infoldings are closely adjacent. Scale bar: 2 μm. (C) Golgi body appearing as a stack of membranous lamellae of increasing width in one direction culminating of a series of vesicles. Scale bar: 0.1 μm. Images demonstrate high quality of tissue preservation with the fixation and preparation procedures used for electron microscopy.

3.1.4. The capillaries

Capillaries passed through the basal layer into the deeper parts of the intermediate and marginal cell layer and tended to be packed with erythrocytes. A narrow layer of basal cells, sometimes only one cell thick, nearly always accompanied the capillary for a short distance into the marginal and intermediate cell layer (not shown). Whichever cell type was in contact with the capillary, and all three cell types could be, it was separated by a well-defined basement membrane and a narrow space containing layers of a material similar to that comprising the basement membrane. Capillary pericytes, where present, were also surrounded by a basement membrane except at their junction with the capillary endothelial cells (Fig. 4A). The capillary endothelial cells have not been seen to be fenestrated in any of the specimens examined, nor has any structure resembling a contractile element been observed. However, the endothelial cells frequently had pinocytic invaginations and coated vesicles associated both with their luminal and exterior walls (Fig. 4A inset).

The overall impression of the SV was of a compact structure comprising three cell types which had widespread cell-to-cell contact via extensive prolongations and interdigitations of their cell membranes. The marginal and intermediate cells possessed large numbers of mitochondria suggesting a highly active tissue. The stria was isolated from the endolymph by tight junctions between the marginal cells and from the capillary lumens by tight junctions between endothelial cells.

3.2. The loop diuretics

Material from six patients was available. One patient (15) had received 1100 mg of Frusemide over a period of 12 hours prior to death. This was equivalent to a dose of 20 mg/kg and was the largest dose administered. None of the patients were in renal failure. SEM showed that the endolymphatic surface of the SV of different patients presented a range of appearances from near normality to moderate disruption. In the least severely affected case the spiral prominence and transitional cells were normal and the SV was either flat or had occasional clusters of adjacent cells showing minimal swelling (Fig. 6A,B). The sporadic findings of cellular swelling were more marked in the basal coil and were almost absent in the SV from the apical regions.

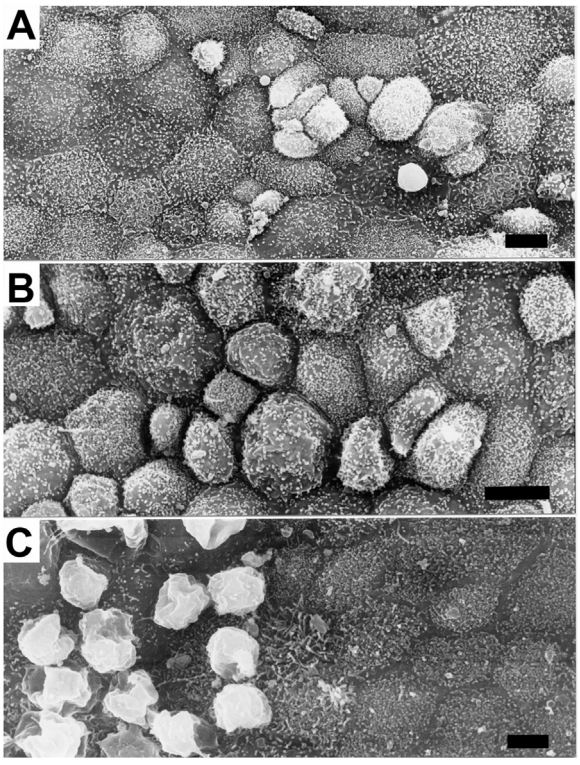

Fig. 6. Effects of loop diuretics on marginal cells, visualised by scanning electron microscopy. (A) Patient 12. (B) Patient 11. (C) Patient 13. Scale bars: 10 μm. All specimens are from the upper basal turn. A variety of changes in the SV following the use of the loop diuretics. Minor swelling of the marginal cells is seen in A whilst gross distortion is present in C. The heterogeneity of the response in an individual is also apparent with normal looking cells next to grossly distorted ones.

In the other five patients a variety of more marked changes was observed. All of the changes were sporadic with apparently

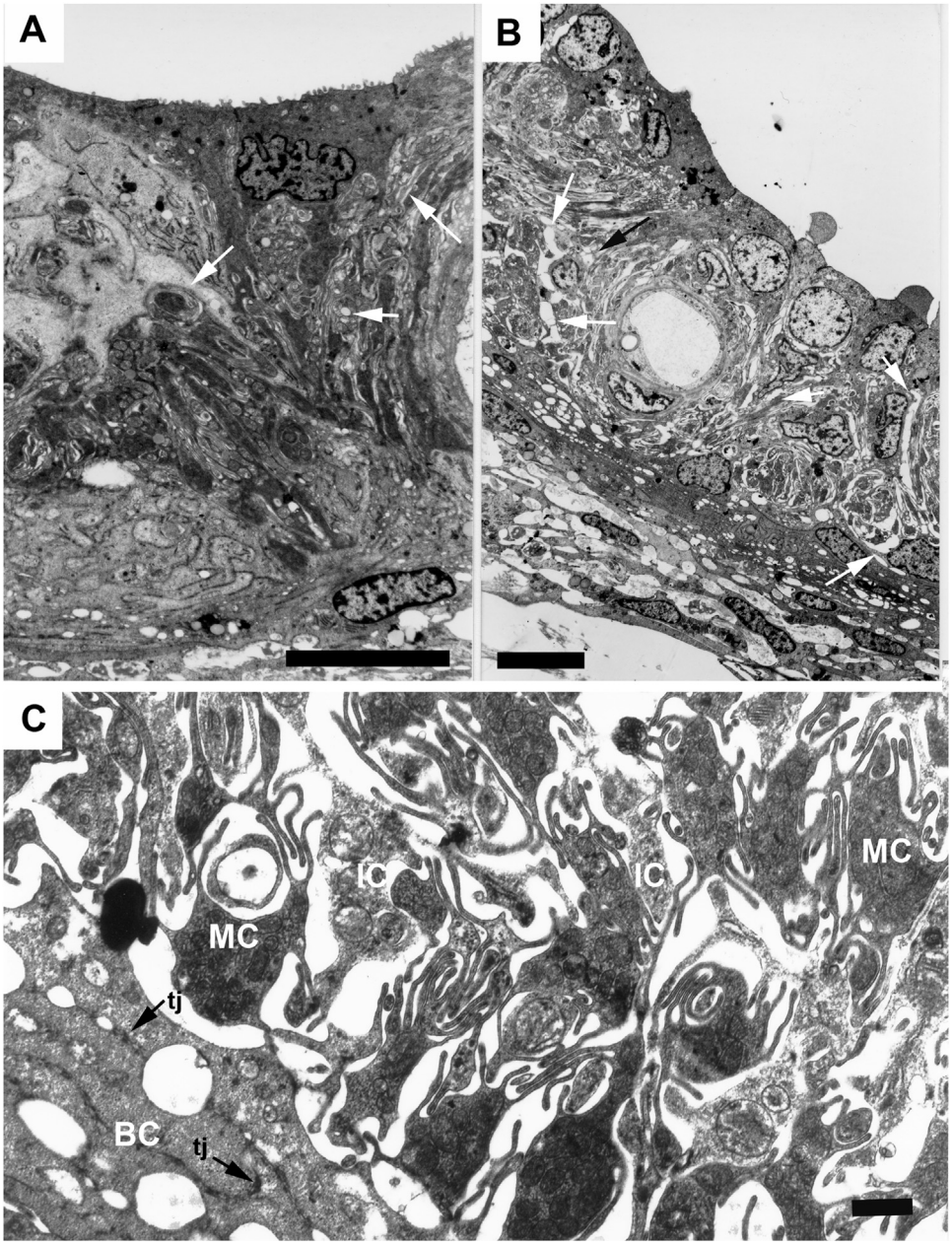

Fig. 7. Effects of loop diuretics on marginal cells, visualised by transmission electron microscopy. (A) Patient 14: mid basal turn. Scale bar 10 μm. (B) Patient 11; lower middle turn. Scale bar: 10 μm. (C) Patient 11; lower middle turn. Scale bar: 1 μm. The least affected stria, panel A, shows only slight changes with small intercellular spaces present between marginal and intermediate cells (arrowed). In the most affected specimen, panels B&C, the endolymphatic surface is blistered, the nuclei of the marginal cells are rounded up and there are large spaces between marginal cells (MC) and intermediate cells (IC) (arrows) (panel B). The formation of the oedematous spaces clearly exposes the extensive infolding basal projections of marginal cells that enclose large mitochondria. Intermediate cells appear shrunken (panel C). Basal cells (BC) appear unaffected without enlarged intercellular spaces between adjacent cells and tight junction-like puncta (tj) are intact (panel C).

normal cells interspersed with cells showing surface changes. The most severe changes are shown in Fig. 6C from the patient who had received the highest doses. Even in this case the patchy nature of the change could be seen with apparently normal cells interspersed with swollen and blistered cells.

TEM showed a range of changes consistent with those seen by SEM. In the least affected, the SV was compact with a smooth endolymphatic surface and the normal range of features seen in the marginal cells. There were narrow spaces between the processes of the marginal and intermediate cells, but it was difficult to decide whether these were secondary to a generalized oedema or to shrinkage of the processes (Fig. 7A). There was no disruption of the tight junctions between marginal cells and the mitochondria were well preserved. The basal cell layer was normal.

In the most affected strial tissue the disruption of the intermediate cell layer became more severe, with large intercellular cystic spaces being seen (Fig. 7B, C). Cystic spaces were also found within the marginal cells and the retraction of the intermediate cells led to condensation of the organelles around the nuclei. The mitochondria were well preserved despite the extensive changes that had otherwise occurred, and the capillaries were intact. Significant enlargement of the intercellular spaces could occur, resulting in marked separation of the cell types from each other (Fig. 7C), but there was no disruption of the basal cell layer with punctate,

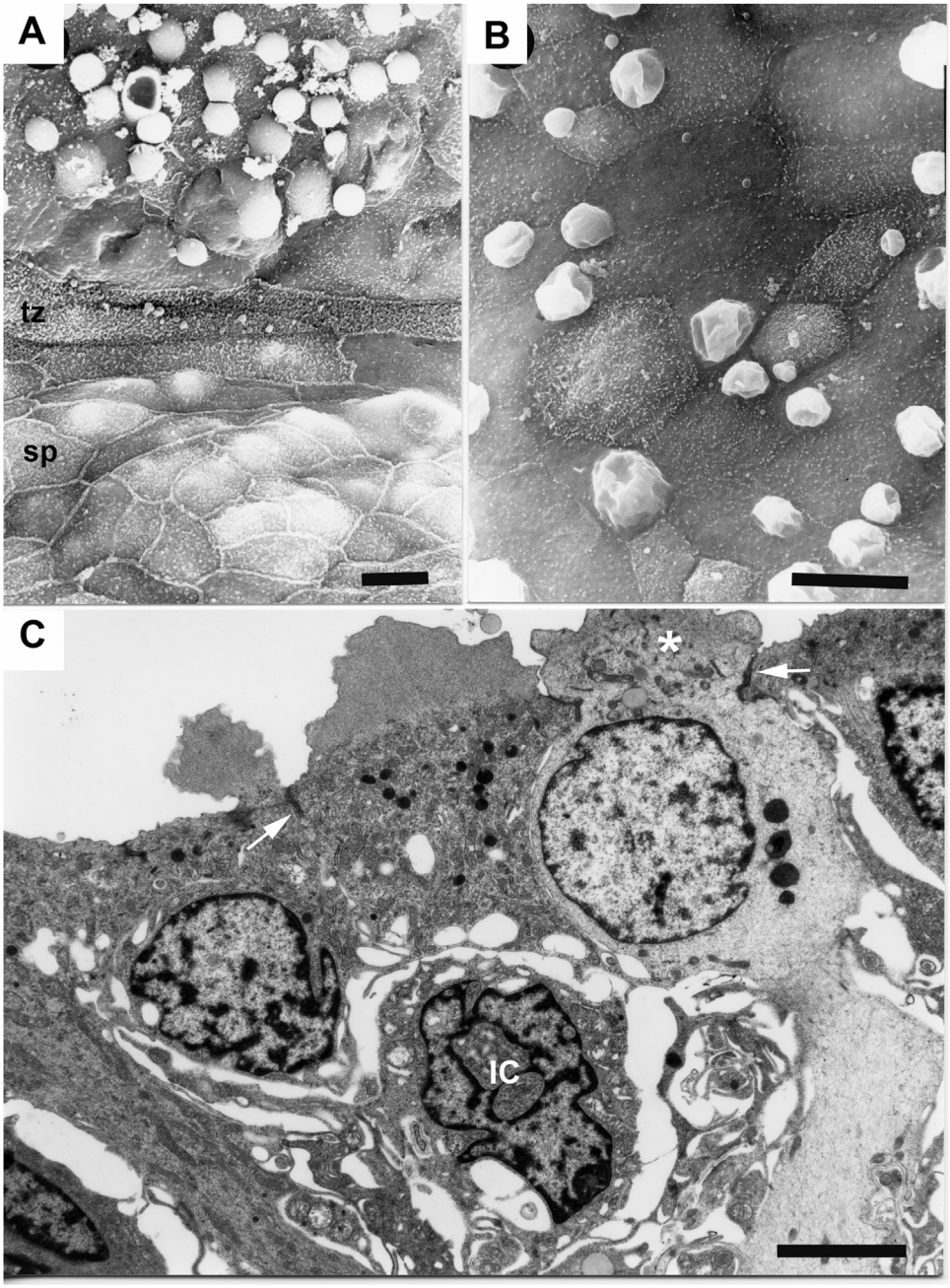

Fig. 8. Aminoglycoside and renal failure. (A) Patient 10; lower middle turn, SEM. Abbreviations: tz = transitional zone; sp = spiral prominence. Scale bar: 10 µm. (B) Patient 9; basal turn, SEM. Scale bar: 10 µm. Marked changes are seen in the SV of both patients, with major loss of the microvilli and the development of surface blisters. The transitional zone and spiral prominence are normal (panel A). (C) Patient 10; lower middle turn, TEM. Scale bar: 5 µm. Some marginal cells (MC) show protrusions containing amorphous material, while in others the protrusion contains seemingly undamaged organelles (asterisk), but tight junctions between adjacent marginal cells are intact (arrows). Some marginal cells also exhibit much reduced cytoplasmic electron density and their nuclei are rounded. Large intercellular spaces are present around intermediate cells (IC) and the cytoplasm of these cells appears condensed.

close appositions between cells, presumably at the tight junctions, preserved. This extensive intercellular oedema in this human specimen closely resembled that seen in the SV of guinea pigs treated with loop diuretic (Forge, 1981a).

3.3. The aminoglycosides

Difficulty was encountered in finding subjects who had received only aminoglycosides during their course of treatment. Both patients in this study were in renal failure and neither had had an audiogram. The SV in both patients showed marked changes (Fig. 8A, B), a normal spiral prominence and transitional zone with marked blistering of the SV itself. The endolymphatic surface of these cells appeared to have relatively few microvilli when compared with those of the control group. These changes whilst present throughout the SV were most marked in the middle of the basal turn.

In sectioned material (Fig. 8C) there was blistering of the endolymphatic surface with the mid-basal sections being most affected. The surface blisters had a limiting bilaminar membrane and were usually filled with a homogeneous matrix although in a few instances, organelles were present in the blister. The tight junctions between neighbouring marginal cells remained intact despite wide separation of other parts of the cell. The contents of the bod-

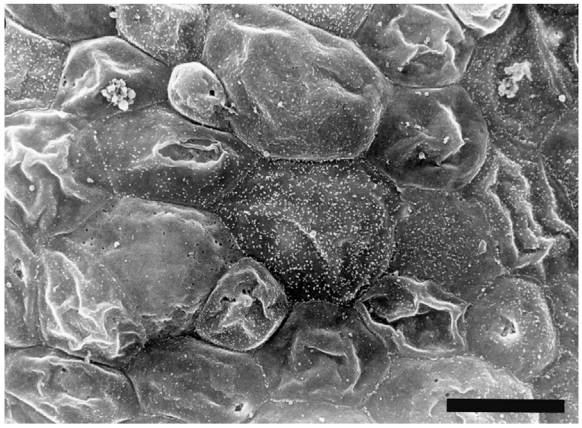

Fig. 9. Effects of aminoglycosides and loop diuretics, visualised by scanning electron microscopy. Patient 19; lower middle turn. Scale bar: 10 µm. There is patchy swelling of the marginal cells with loss of microvilli and blistering of the surface. Even in such an affected stria, occasional marginal cells appear normal.

ies of the marginal cells were not different from those seen in the controls. The wide intercellular spaces between marginal and intermediate cells appeared to be due to shrinkage of the processes of the intermediate cells, as the organelles in these cells were tightly packed and the processes of the cells were clearly defined as thin, often curled fingers limited by an intact membrane. The basal cells were not affected but the capillaries tended to be empty of erythrocytes (not shown).

3.4. The aminoglycosides and loop diuretics

The patients receiving both drugs tended to be severely ill for a long time before their deaths. There was a general similarity amongst the surface features of the SV of all five patients despite the fact that three were in renal failure. In all, the spiral prominence and transitional zone were normal throughout the cochlea, although there were varying degrees of change in the SV. This change was a patchy swelling of the endolymphatic surface of many of the marginal cells. Not all the cells were swollen, but those that were had a rather smooth swelling with a loss of microvilli (Fig. 9). The changes were less marked in the apical coil.

In one patient the SV was compact and was architecturally almost normal with only small cystic spaces being found in the body of the tissue (Fig. 10A). However, there was a marked decrease in the thickness in the luminal-ligament direction in the central region of the SV (arrows in Fig. 10A). The SV was normally about 30 µm thick, as at the right hand side of Fig. 10A, whereas it was ca, 20 µm thick at the point delimited by the arrows. A similar reduction in SV thickness following aminoglycoside treatment in healthy animals has been reported (Forge et al., 1987).

In the other four cases the apical surface of the marginal cells was irregular with protrusions and loss of microvilli, as represented in Fig. 10B. The apical cystic spaces found in those patients in renal failure who had been given loop diuretics were not seen; rather a generalised protrusion of the cell surface which was filled with cytoplasm. The apical cytoplasm was not however normal in that it contained small, membrane-bound, cystic spaces and the nuclei tended to be rounded-up rather than multilobulated as in the controls. As a group, the marginal cells were quite compact with minimal separation of their cell bodies and intact tight junctions, but many had reduced cytoplasmic staining density, and the complex basal projections appeared to have been lost so the cells had a more regular outline. Intercellular separation appeared to be limited to intermediate/basal cell layer with sometimes quite large spaces being apparent. Many of the intermediate cells were shrunken with the cytoplasm compacted around the nuclei (Fig. 10B). These findings bear a close resemblance to those seen with the loop diuretics alone.

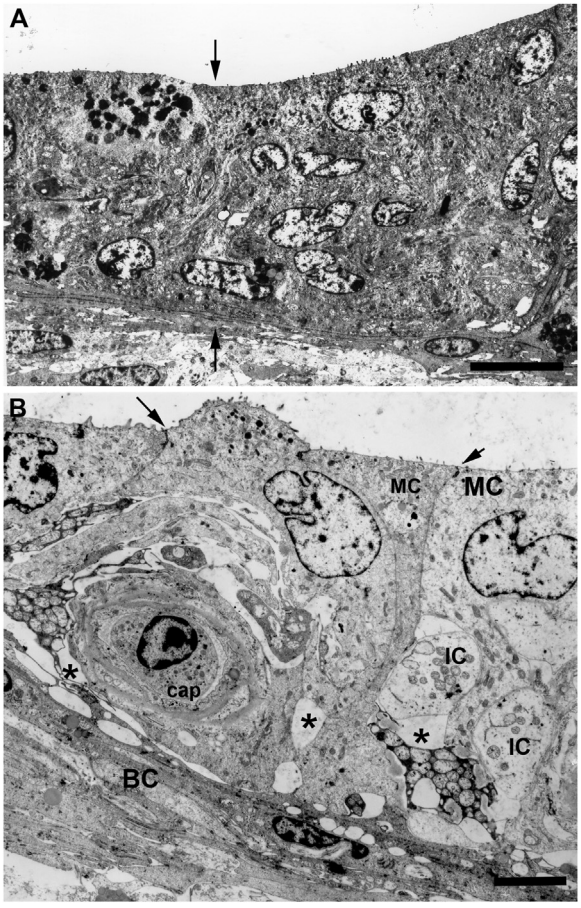

Fig. 10. Effects of aminoglycosides and loop diuretics, visualised by TEM. (A) Patient 20; lower middle turn. Scale bar: 10µm. There is a clear reduction in the thickness of the stria (luminal surface to basal cell-spiral ligament interface) at the site indicated by the two arrows, and some apparent cellular re-organization. (B) Patient 21; apical turn. Scale bar: 5µm. There are apical protrusions from the marginal cells. Some marginal cells show reduced cytoplasmic density and an apparent loss of the basal infoldings. Tight junctions between marginal cells (arrowed) are intact. Enlarged intercellular spaces within the body of the stria are evident (asterisks). Basal cell layer (BC) is undisturbed.

Overall, the stria appeared to have been markedly disrupted by the combination of an aminoglycoside and a loop diuretic, especially in the presence of renal failure. The changes were however different from those seen with the loop diuretics alone.

4. Discussion

One of the major problems with the study of human material has been the avoidance of post mortem autolysis artefact – “a cause de la difficulte de se procurer des preparations fraiches” (Corti, 1851). This constraint still exists and means that in order to allow structural changes in human tissues to be ascribed to pathology rather than post mortem autolysis, then some internal tissue marker must be seen to be normal in the specimens examined. Mitochondria are fairly good indicators of the degree of post-mortem delay in fixation (Trump et al., 1965; Ghadilly, 1980), and in this study the preservation of normal or near normal mitochondrial morphology, and that of other intracellular organelles as assessed at high resolution, was required before the tissue from any individual was included. Further support for the adequacy of fixation comes from the work of Kimura and Schuknecht (1970a,b) where

operative specimens of the basal stria were obtained from profoundly deaf patients. They thought that this SV showed normal features and their micrographs cannot be distinguished from those of the control specimens in this study. Thus, it seems reasonable to ascribe the changes seen in the treated groups in this study to the effects of the administered drugs or the intercurrent illness or both.

Loop diuretics inhibit the action of the sodium-potassium symporter NKCC2 (Na^+-K^+-$2Cl^-$) that, as well as in the ascending limb of the loop of Henle in the kidney, is present at high levels in the plasma membranes of the infoldings of the marginal cells (Ding et al., 2016). In concert with $Na^{+-}K^+$-ATPase, which is also present at high levels in the membrane of marginal cell infoldings (Ding et al., 2016), the symporter is responsible for the uptake K^+ into marginal cells from the intercellular spaces of the stria. The numerous large mitochondria within the marginal cell infoldings provide energy for active ion transport. K^+ is released into the intercellular spaces at high concentration from the intermediate cells by an electrogenic mechanism that generates endocochlear potential (EP), the high positive electrical potential recorded in cochlear endolymph (Salt et al., 1987; Steel and Barkway, 1989). The tight junctions between marginal cells, between capillary endothelial cells and extensively between adjacent basal cells provide the barriers that confine the high K^+ to the SV and prevent dissipation of the electrical potential. The inhibition of NKCC2 by the loop diuretic blocks the uptake of K^+ into marginal cells such that the ion accumulates to high concentration in the intercellular space of the stria, thereby drawing in fluid by osmosis leading to the swelling of the tissue and separation of the normally closely apposed cells (Ding et al., 2016). The maintenance of the tight junctions all around the intercellular compartment of the stria confines the ions and fluid to the intercellular spaces of the stria. The physiological consequence is a rapid fall in EP, and functionally in hearing impairment. In healthy animals given high doses of a loop diuretic, the structural changes in the stria and the physiological and functional consequences are transient, the stria returning to normal morphology, and a high positive EP re-established within hours (Bosher, 1980). In normal clinical use, loop diuretics cause temporary hearing loss, so it seems reasonable to suppose that normally the structural effects on the stria reported here are transient and resolve within a short time.

In experimental work investigating the effects of a loop diuretic on the surface features of the rodent SV, the spiral prominence and transitional zone have always remained unaltered despite severe changes in the stria (Quick and Duvall, 1970; Horn et al., 1977; Forge, 1980). Thus, in addition to the state of the mitochondria, the appearance of the spiral prominence and transitional zone can be taken as a further internal control to assess the quality of preservation. Changes in the surface features of these two structures would suggest a defect in technique and make evaluation of the SV unreliable. In all the specimens examined, the spiral prominence and transitional zone did not differ from the appearance seen in animal studies where preservation was known to be good.

In the group that received the loop diuretics alone, renal failure as measured by plasma urea and creatinine levels was absent, although all but one of the patients were retaining fluid because of cardiac insufficiency. In this group the changes seen were difficult to distinguish from those seen in animal studies where loop diuretics were given to healthy animals (Bosher et al., 1973; Brummett et al., 1977; Horn et al., 1977; Forge, 1980; Pike and Bosher, 1980). Various doses and routes of administration were prescribed for the patients and these varied from longstanding oral treatment with bumetanide to rapidly given, large intravenous doses shortly before death. The surface features do not always indicate the extent of the changes in the underlying cell types. However, the changes in the intermediate cell layer with shrinkage of the cell processes, the formation of large cystic intercellular spaces and, in the most severely affected individuals, bulging of the marginal cells with loss of surface microvilli are almost indistinguishable from those seen in guinea pigs (Forge, 1981b, a) or rats (Bosher, 1980).

Renal failure was not present in the patients described here and so, unlike Arnold's study (Arnold et al., 1981), the effects can very probably be ascribed to the loop diuretics. Fluid retention was however present, and it is possible that this might have contributed to the changes. Nevertheless, this study was designed to determine whether the changes seen in humans resembled those seen in animals and since the loop diuretics are nearly always given for fluid retention then the combination of the two is an inescapable factor when human material is studied. It therefore seems reasonable both to accept that the morphological findings from healthy animals given large doses of loop diuretics are similar to those seen in unhealthy fluid retaining humans, and to continue to use animals as a model for predicting a clinical effect in humans.

The SV from the 7 patients in the other treatment groups (aminoglycosides only, two patients; aminoglycosides and loop diuretics, five patients) showed a wide range of appearances. Where renal function was normal and the dose of loop diuretics was small the SV had minimal or no change. With renal failure several changes were seen in the SV that could not be ascribed to the concurrent administration of the loop diuretics. There was patchy swelling of the marginal cells and a widening of the intercellular spaces especially in the intermediate/basal cell region with shrinkage of the intermediate cell processes in some specimens.

There are few ultrastructural studies of the SV in renal failure in man or experimental animals. Arnold described the SV in two cases of Alport's syndrome which is an autosomal dominant condition with renal failure and deafness (Arnold, 1980). There was blistering of the endolymphatic surface of the SV clearly seen in semi-thin sections and large intercellular spaces between the intermediate cells with apparent shrinkage of their processes. That tissue was well fixed and the appearances are indistinguishable from those seen in the current work. An animal study from rats made uraemic by subtotal nephrectomy was performed by Merck and colleagues (Merck et al., 1976). They found strial thickening with opening of the intercellular spaces between the intermediate cell processes. The marginal cells appeared relatively normal although the mitochondria were swollen. Their micrographs are difficult to distinguish from those of Arnold (1980) and those presented here, suggesting that renal failure both in man and the rat exerts a strong influence on the SV which is presumably a major part of the mechanism for the hearing loss sometimes seen in this condition. The pattern of response of the SV in the face of renal failure or the administration of the loop diuretics is remarkably similar and is presumably the morphological expression of the results of the SV's attempt to maintain the integrity of the endolymph despite the 'toxic' action of the uraemia or the loop diuretics on its metabolism.

Structural changes have been seen in the SV of experimental animals treated with the aminoglycosides. Both after repeated daily injections in guinea pigs, and after a single dose of aminoglycoside accompanied by a diuretic in mice, there is significant reduction in SV thickness, between the luminal surface and the basal cell-spiral ligament interface (Forge and Fradis, 1985; Forge et al., 1987; Taylor et al., 2008). This is mainly the consequence of reductions in volume fraction occupied by marginal cells resulting in part from a loss in their basal infoldings. These observations are remarkably similar to what has been observed in the present study. In animals, the effects on the SV become more pronounced with time so that the tissue may become severely atrophied (Taylor et al., 2008). This would suggest that the effects of

aminoglycoside treatment on SV structure observed in the present study of the human tissue do not resolve. The marginal cells appear to undergo a marked and progressive shrinkage following chronic gentamicin treatment. In the present study minor changes affecting the cytoplasm of the apex of the marginal cells with the formation of small vacuoles were seen in some of the patients receiving aminoglycosides but were overshadowed by the changes attributable to the loop diuretics, renal failure or both.

5. Conclusion

The patterns of structural changes seen in the SV of sick humans strongly resemble those seen in healthy experimental animals given large doses of the loop diuretics or aminoglycosides. It therefore seems reasonable to use experimental animals to predict a toxic effect in humans, although the lack of toxicity in any animal species cannot ensure safety in humans because of the large variations in the way that animals from different orders metabolise various drugs.

Declaration of Competing Interest

The authors declare no competing financial interests.

CRediT authorship contribution statement

Anthony Wright: Conceptualization, Data curation, Formal analysis, Funding acquisition, Investigation, Methodology, Project administration, Resources, Software, Supervision, Validation, Visualization, Writing – original draft, Writing – review & editing. **Andrew Forge:** Conceptualization, Data curation, Formal analysis, Funding acquisition, Investigation, Methodology, Project administration, Resources, Software, Supervision, Validation, Visualization, Writing – original draft, Writing – review & editing. **Daniel J. Jagger:** Conceptualization, Data curation, Formal analysis, Funding acquisition, Investigation, Methodology, Project administration, Resources, Software, Supervision, Validation, Visualization, Writing – original draft, Writing – review & editing.

Data availability

Data will be made available on request.

Acknowledgments

This work was supported by a UK Medical Research Council Clinical Research Fellowship to AW.

References

Arnold, W, 1980. [Considerations on the pathogenesis of the cochleo-renal syndrome (author's transl)]. Acta Otolaryngol. 89, 330–341.
Arnold, W, Nadol Jr., JB, Weidauer, H, 1981. Ultrastructural histopathology in a case of human ototoxicity due to loop diuretics. Acta Otolaryngol. 91, 399–414.
Bosher, SK, 1980. The nature of the ototoxic actions of ethacrynic acid upon the mammalian endolymph system. II. Structural-functional correlates in the stria vascularis. Acta Otolaryngol. 90, 40–54.
Bosher, SK, Smith, C, Warren, RL, 1973. The effects of ethacrynic acid upon the cochlear endolymph and stria vascularis. A preliminary report. Acta Otolaryngol. 75, 184–191.
Brummett, R, Smith, CA, Ueno, Y, Cameron, S, Richter, R, 1977. The delayed effects of ethacrynic acid on the stria vascularis of the guinea pig. Acta Otolaryngol. 83, 98–112.
Corti, A, 1851. Reserches sur l'organe de l'ouie des mammifieres. Zeitschrift fur Wissenschaftliche Zoologie 3, 109–171.
Ding, D, Liu, H, Qi, W, Jiang, H, Li, Y, Wu, X, Sun, H, Gross, K, Salvi, R, 2016. Ototoxic effects and mechanisms of loop diuretics. J. Otol. 11, 145–156.
Forge, A, 1980. The endolymphatic surface of the stria vascularis in the guinea-pig and the effects of ethacrynic acid as shown by scanning electron microscopy. Clin. Otolaryngol. Allied Sci. 5, 87–95.
Forge, A, 1981a. Ultrastructure in the stria vascularis of the guinea pig following intraperitoneal injection of ethacrynic acid. Acta Otolaryngol. 92, 439–457.
Forge, A, 1981b. Electron microscopy of the stria vascularis and its response to etacrynic acid. A study using electron-dense tracers and extracellular surface markers. Audiology 20, 273–289.
Forge, A, Fradis, M, 1985. Structural abnormalities in the stria vascularis following chronic gentamicin treatment. Hear. Res. 20, 233–244.
Forge, A, Schacht, J, 2000. Aminoglycoside antibiotics. Audiol. Neurootol. 5, 3–22.
Forge, A, Wright, A, Davies, SJ, 1987. Analysis of structural changes in the stria vascularis following chronic gentamicin treatment. Hear. Res. 31, 253–265.
Ghadilly, FN, 1980. Diagnostic electron microscopy of tumours. Butterworths, London.
Hawkins, JE, 1976. Drug ototoxicity. In: Keidel WDaN, W.D. (Ed.), Handbook of Sensory Physiology. Springer Verlag, Berlin, pp. 707–748.
Hawkins Jr., JE, Lurie, MH, 1953. The ototoxicity of dihydrostreptomycin and neomycin in the cat. Ann. Otol. Rhinol. Laryngol. 62, 1128–1148.
Hawkins Jr., JE, Stebbins, WC, Johnsson, LG, Moody, DB, Muraski, A, 1977. The patas monkey as a model for dihydrostreptomycin ototoxicity. Acta Otolaryngol. 83, 123–129.
Horn, KL, Langley, LR, Gates, GA, 1977. Effect of ethacrynic acid on the stria vascularis. Arch. Otolaryngol. 103, 539–541.
Jagger, DJ, Forge, A, 2015. Connexins and gap junctions in the inner ear–it's not just about K(+) recycling. Cell Tissue Res. 360, 633–644.
Kimura, RS, Schuknecht, HF, 1970a. The ultrastructure of the human stria vascularis. II. Acta Otolaryngol. 70, 301–318.
Kimura, RS, Schuknecht, HF, 1970b. The ultrastructure of the human stria vascularis. I. Acta Otolaryngol. 69, 415–427.
Matz, GJ, 1976. The ototoxic effects of ethacrynic acid in man and animals. Laryngoscope 86, 1065–1086.
Matz, GJ, Beal, DD, Krames, L, 1969. Ototoxicity of ethacrynic acid. Demonstrated in a human temporal bone. Arch. Otolaryngol. 90, 152–155.
McGee, TM, 1961. Streptomycin sulfate and dihydrostreptomycin toxicity. Trans. Am. Acad. Ophthalmol. Otolaryngol. 65, 222–229.
Merck, W, Hoppe-Seyler, G, Curten, I, 1976. [Ultrastructural changes of the stria vaseularis and the spiral ligament in chronic uremic rats (author's transl)]. Arch. Otorhinolaryngol. 214, 63–70.
Meriwether, WD, Mangi, RJ, Serpick, AA, 1971. Deafness following standard intravenous dose of ethacrynic acid. JAMA 216, 795–798.
Pike, DA, Bosher, SK, 1980. The time course of the strial changes produced by intravenous furosemide. Hear. Res. 3, 79–89.
Quick, CA, Duvall 3rd, AJ, 1970. Early changes in the cochlear duct from ethacrynic acid: an electronmicroscopie evaluation. Laryngoscope 80, 954–965.
Robinson, DW, Sutton, GJ, 1979. Age effect in hearing - a comparative analysis of published threshold data. Audiology 18, 320–334.
Salt, AN, Melichar, I, Thalmann, R, 1987. Mechanisms of endocochlear potential generation by stria vascularis. Laryngoscope 97, 984–991.
Shambaugh Jr., GE, Derlacki, EL, Harrison, WH, House, H, House, W, Hildyard, V, Schuknecht, H, Shea, JJ, 1959. Dihydrostreptomycin deafness. J. Am. Med. Assoc. 170, 1657–1660.
Souter, M, Forge, A, 1998. Intercellular junctional maturation in the stria vascularis: possible association with onset and rise of endocochlear potential. Hear. Res. 119, 81–95.
Steel, KP, Barkway, C, 1989. Another role for melanocytes: their importance for normal stria vascularis development in the mammalian inner ear. Development 107, 453–463.
Taylor, RR, Nevill, G, Forge, A, 2008. Rapid hair cell loss: a mouse model for cochlear lesions. J. Assoc. Res. Otolaryngol. 9, 44–64.
Trump, BF, Goldblatt, PJ, Stowell, RE, 1965. Studies on Necrosis of Mouse Liver in Vitro. Ultrastructural Alterations in the Mitochondria of Hepatic Parenchymal Cells. Lab. Invest. 14, 343–371.
Wright, A, 1980a. Scanning electron microscopy of the human cochlea–postmortem autolysis artefacts. Arch. Otorhinolaryngol. 228, 1–6.
Wright, A, 1980b. Scanning electron microscopy of the human cochlea - the stria vascularis. Arch. Otorhinolaryngol. 229, 39–44.
Zhang, W, Dai, M, Fridberger, A, Hassan, A, Degagne, J, Neng, L, Zhang, F, He, W, Ren, T, Trune, D, Auer, M, Shi, X, 2012. Perivascular-resident macrophage-like melanocytes in the inner ear are essential for the integrity of the intrastrial fluid-blood barrier. Proc. Natl. Acad. Sci. U. S. A. 109, 10388–10393.